ELSEVIER

Biochimica et Biophysica Acta 1457 (2000) 129–144

BIOCHIMICA ET BIOPHYSICA ACTA
BBA

www.elsevier.com/locate/bba

Salt shock-inducible Photosystem I cyclic electron transfer in *Synechocystis* PCC6803 relies on binding of ferredoxin:NADP$^+$ reductase to the thylakoid membranes via its CpcD phycobilisome-linker homologous N-terminal domain

Jasper J. van Thor [a,e], Robert Jeanjean [b], Michel Havaux [c], Klaas A. Sjollema [d], Francoise Joset [b], Klaas J. Hellingwerf [a], Hans C.P. Matthijs [e,*]

[a] *E.C. Slater Institute, University of Amsterdam, Nieuwe Achtergracht 127, 1018 WS Amsterdam, The Netherlands*
[b] *LCB-CNRS, 31 Chemin J. Aiguier, 13402 Marseille Cedex 20, France*
[c] *CEA/Cadarache, DEVM, 13108 St Paul-lez-Durance, France*
[d] *Laboratory for Electron Microscopy, University of Groningen, P.O. Box 14, 9750 AA Haren, The Netherlands*
[e] *ARISE/MB, University of Amsterdam, Nieuwe Achtergracht 127, 1018 WS Amsterdam, The Netherlands*

Received 29 November 1999; accepted 24 January 2000

Abstract

Relative to ferredoxin:NADP$^+$ reductase (FNR) from chloroplasts, the comparable enzyme in cyanobacteria contains an additional 9 kDa domain at its amino-terminus. The domain is homologous to the phycocyanin associated linker polypeptide CpcD of the light harvesting phycobilisome antennae. The phenotypic consequences of the genetic removal of this domain from the *petH* gene, which encodes FNR, have been studied in *Synechocystis* PCC 6803. The in frame deletion of 75 residues at the amino-terminus, rendered chloroplast length FNR enzyme with normal functionality in linear photosynthetic electron transfer. Salt shock correlated with increased abundance of *petH* mRNA in the wild-type and mutant alike. The truncation stopped salt stress-inducible increase of Photosystem I-dependent cyclic electron flow. Both photoacoustic determination of the storage of energy from Photosystem I specific far-red light, and the re-reduction kinetics of P700$^+$, suggest lack of function of the truncated FNR in the plastoquinone–cytochrome b_6f complex reductase step of the PS I-dependent cyclic electron transfer chain. Independent gold-immunodecoration studies and analysis of FNR distribution through activity staining after native polyacrylamide gelelectrophoresis showed that association of FNR with the thylakoid membranes of *Synechocystis* PCC 6803 requires the presence of the extended amino-terminal domain of the enzyme. The truncated Δ*petH* gene was also transformed into a NAD(P)H dehydrogenase (NDH1) deficient mutant of *Synechocystis* PCC 6803 (strain M55) (T. Ogawa, Proc. Natl. Acad. Sci. USA 88 (1991) 4275–4279). Phenotypic characterisation of the double mutant supported our conclusion that both the NAD(P)H dehydrogenase complex and FNR contribute independently to the quinone cytochrome b_6f reductase step in PS I-dependent cyclic electron transfer. The distribution, binding properties and function of FNR in the model cyanobacterium *Synechocystis* PCC 6803 will be discussed.

Abbreviations: DCMU, 3-(3,4-dichlorophenyl)-1,1-dimethylurea; FNR, ferredoxin:NADP$^+$ reductase; PAM, pulse amplitude modulation; NDH, NAD(P)H dehydrogenase complex; PS, Photosystem

* Corresponding author. Fax: +31-20-525-7056; E-mail: a417hcpm@chem.uva.nl

0005-2728/00/$ – see front matter
PII: S0005-2728(00)00072-4

Keywords: Ferredoxin:NADP$^+$ reductase; Cyclic electron transport; Photosystem I; Green fluorescent protein; *petH*; (*Synechocystis* PCC 6803)

1. Introduction

Cyanobacteria are prokaryotic organisms that primarily perform oxygenic photosynthesis. Transfer of electrons from water to NADP$^+$ involves Photosystem II (PS II), Photosystem I (PS I) and an electron transfer chain that interconnects these two photosynthetic reaction centres in a linear fashion. Like green plants and eukaryotic algae, cyanobacteria also perform photosynthetic electron transfer, which is cyclic in nature and (light-) driven by PS I only. In the mode of cyclic operation, electrons are transferred from the lumen to the stroma across the thylakoid membrane by PS I photochemistry and return from the stromal side to the lumenal side of PS I via a chain of electron transfer carriers (for a recent review see [1]). It has been demonstrated that ferredoxin, the plastoquinone pool, the cytochrome b_6f complex, and the lumenal electron carriers (plastocyanin and/or cytochrome c_6) are used in common between linear and cyclic electron transfer [1]. These components (with the exception of ferredoxin and plastocyanin) also take part in thylakoid membrane-based dark respiratory electron transfer, which is accomplished in cyanobacteria as well (for a review see [2]). Influx of electrons from stromal donors into the respiratory chain is mediated by a bacterial NDH1 complex in the thylakoid membrane [2]. The particular complex also supplies electrons for PS 1 driven cyclic electron transfer in addition to the ferredoxin mediated plastoquinone reduction pathway [1].

During linear electron transfer the turnover rates for PS I in cyanobacteria range from 35 to 140 s^{-1} [3]. This number stems from measurement of the rate of re-reduction of the PS1 centre P700$^+$ in the dark period, which follows upon full P700 oxidation in actinic white light. It was noted that the P700$^+$ re-reduction rates, after selective illumination and full oxidation of PS I with far-red light (>710 nm) were much slower (± 4 s^{-1}) for cyanobacteria and green algae in [3]. Those slower kinetics in far-red light likely reflect the differences in the mechanism of reduction of the plastoquinone-pool and/or the cytochrome b_6f complex. This occurs relatively fast if electrons are supplied from PS II in white light, and slow if supply is from the stroma as occurs in far-red PS I light or in white light in presence of the PS II inhibitor DCMU. In subsequent electron transfer, the rates of steps involved in the reduction of P700$^+$ from plastoquinone were determined directly in vivo for a thermophilic *Synechococcus* species [4]. The slowest rate was the reduction of the Rieske protein by plastoquinone (~ 500 s^{-1}). All subsequent reactions were observed to proceed at faster rates [4]. It is thus concluded that electron donation from the stroma to the plastoquinone pool or cytochrome b_6f complex is by far the slowest and has the highest control on the flux of cyclic electron transfer in vivo. An independent and basically different assay method, photo-acoustic monitoring of the efficiency of light energy transformation, supported these observations. The photo-acoustic method monitors the quantum efficiency during steady state turnover of electrons, in contrast to the non-steady state P700$^+$ re-reduction assay. Nevertheless, both techniques have been demonstrated to record the 'efficiency' of PS I-dependent cyclic electron flow and its rate limitation in a compatible fashion [5,6].

In chloroplasts, the NDH1 complex has recently been implicated in the reduction of plastoquinone [7,8]. The rates of NAD(P)H oxidation, are not as high as the, earlier documented, ferredoxin-dependent cyclic electron transfer rates [1].

However, in *Synechocystis* PCC 6803 reduction of the plastoquinone-pool and the cytochrome b_6f complex in the dark is predominantly taking place by oxidation of NADPH, which is mediated by a bacterial NDH1 complex in the thylakoid membrane [9]. A mutant of *Synechocystis* PCC 6803 lacking NdhB (designated M55), and therefore lacking functional NAD(P)H dehydrogenase, was found to show a dramatically decreased rate of dark respiration and of P700$^+$ re-reduction (after prior oxidation with far-red light). It was therefore concluded that the stromal oxidation of NADPH constitutes the largest contribution to PS I-dependent cyclic electron transfer and respiratory activity [9–11]. This mutant was

also defective in uptake of inorganic carbon, when present at low concentration [9]. It was recently shown that salt-induced increased capacity of PS I-dependent cyclic electron transfer coincides with recovery of the ability for this mutant to grow in media containing a low concentration of inorganic carbon (0.03% (v/v) CO_2 in air) [12]. It appeared that even in the absence of the NDH1 complex, salt stress induces PS I-dependent cyclic electron transfer [12]. Salt stress induces over-expression of quite some proteins in *Synechocystis* PCC6803 [13], of these proteins flavodoxin may play a role in the inducible increase of PS 1 cyclic electron flow capacity [14]. Over-expression of FNR in *Synechocystis* PCC6803 has also been established as a consequence of salt stress [15].

In chloroplasts, participation of FNR in PS I-dependent cyclic electron transport has been suggested by the inhibitory effect of sulfhydryl-modifying agents (that are known to inhibit the interaction between ferredoxin and FNR) [6,16], and heparin [17]. Though still controversial, FNR may contribute to ferredoxin:quinone-oxidoreductase activity (FQR), by catalysis of 'reverse' electron transfer from NADPH to ferredoxin, or flavodoxin, with NADPH as electron donor, in which case high NADPH:$NADP^+$ and Fd(ox):Fd(red) ratios are needed [1]. A NADPH:plastoquinone reductase function, essentially equivalent to the reaction catalysed by the NDH1 complex, has been proposed for FNR in vegetative cells and heterocysts of the cyanobacterium *Anabaena* sp. [18,19].

Here we provide evidence, based on molecular, genetic and physiological analysis that a part of the FNR pool is directly involved in the rate-limiting step of PS I cyclic electron transfer. FNR does so in addition to the earlier documented contributions of ferredoxin and NADPH dehydrogenase. An essential role for the amino-terminal extension of FNR which as till now is uniquely present in all out of four tested cyanobacteria is proposed from the work presented. It became evident that only the particular FNR function in PS I cyclic electron transfer requires the extended N-terminal domain. It is suggested that the function in PS I cyclic electron transfer likely goes hand in hand with the association between FNR and the thylakoid membranes. The presence of FNR in physically separated pools with different function in *Synechocystis* will be discussed. The traditionally accepted function of FNR ($NADP^+$ reduction in linear photosynthetic electron transport) earlier proved to remain unaffected by the truncation [20].

2. Materials and methods

2.1. Media and culture conditions

Wild-type *Synechocystis* PCC6803 and mutant strains derived thereof were cultured in BG-11 medium at 34°C, under continuous illumination using two TL tubes, which provided an average light intensity of 70 μE m^{-2} s^{-1} [21]. Transformations were performed as described previously [22]. Mutant M55 was grown in medium supplemented with 50 μg/ml kanamycin and 10 mM $NaHCO_3$ [9]. Transformants were selected on BG-11 medium containing 1.5% (w/v) agar (Difco) plates, supplemented with 10 mM $NaHCO_3$, 10 mM *N*-Tris[hydroxymethyl]-2-aminoethanesulfonic acid (TES)/KOH (pH 8.2), 0.3% sodium thiosulfate and either 10 μg/ml streptomycin or 50 μg/ml kanamycin, depending on the antibiotic resistance cassette that was used. A salt-stressed culture was obtained by the addition of NaCl to a final concentration of 0.55 M to a photoautotrophically growing culture [15]. For the analysis of salt-adapted cultures, cells were harvested 12–16 h after the addition of NaCl.

2.2. RNA and DNA analysis

For the isolation of total RNA from *Synechocystis* 6803 suitable for Northern analysis, the RNeasy spin column protocol (Qiagen) was adapted. Cells (10–20 ml of $OD_{750} = 1$) were collected by centrifugation and resuspended in 600 μl lysis-buffer containing 1% β-mercaptoethanol (Qiagen). Alternatively, this buffer could be substituted by 4.5 M guanidinium isothiocyanate (Fluka), 2% (w/v) sodium-*N*-laurylsarcosine (Sigma), 1% (v/v) β-mercaptoethanol and 50 mM Tris–HCl (pH 7.5). There was no need for additional homogenization when this protocol was used. 600 μl of phenol/chloroform (1:1) (equilibrated with Tris–HCl, pH 7.5) was added, mixed and incubated at 65°C for 5 min. The sample was centrifuged, and

the aqueous phase was extracted with chloroform. Next, 600 μl of 70% ethanol was added to the sample, and the RNA was isolated according to the specified protocol (Qiagen). Typical yields were 50–200 μg RNA. Northern hybridisation with a *Synechocystis petH* probe was performed as described previously [15].

DNA was isolated by adapting a glass-milk kit (Pharmacia). Utilising the specific DNA binding properties of silica-gel particles, DNA was purified from peptidoglycan contaminations. A cell suspension was lysed with lysozyme and digested with RNAse and Proteinase K, and was extracted with phenol twice. Subsequently, 2 volumes of a buffer containing 6 M NaI and 50 mM Tris–HCl (pH 8.0) was added (gel-solubilisation buffer; Pharmacia), and DNA was purified by gentle handling of the glass-milk particles, with elution of the DNA at 50°C.

2.3. Construction of the 5′-truncated petH gene

The *Synechocystis* PCC 6803 *petH* gene was cloned on a 2.9 kbp *Bam*HI/*Hin*dIII fragment, resulting in pSP35-9 [15]. The truncation of 75 amino acid residues of the N-terminus of PetH required the in-frame deletion of 225 bp. This was achieved with a loop-out mutagenesis strategy, combined with negative selection against the non-mutagenised, uracil-containing, complementary strand produced by the *dut ung Escherichia coli* strain CJ236 [23]. To this end, a 830 bp *Eco*RI/*Sma*I fragment from pSP35-9 was cloned in M13mp19. U-DNA from this construct was isolated from *E. coli* CJ236. The loop-out oligonucleotide SPETTRUNC (5′-GGAGCAATTAACCCATGGAGGGAGATTCGCCTT-3′) was phosphorylated and annealed to the template. Subsequent second-strand synthesis and transformation yielded clones with the correctly reduced size of the *Eco*RI/*Sma*I insert. The 605 bp insert was sequenced and cloned into the 5.5 kbp *Eco*RI/*Sma*I fragment from pSP35-9, resulting in construct pSP35-9Δ. The Ω cassette, encoding streptomycin and spectinomycin resistance, was cloned as a 2.0 kbp *Bam*HI fragment from pHP45Ω [24] in the *Bam*HI site of pSP35-9Δ, producing pSP35-9ΔΩ. A fragment encoding the CpcD-homologous N-terminal domain of PetH and 213 bp untranslated region of pSP35-9 was cloned as a 437 bp *Xba*I/*Spe*I fragment from pSP35-9 into the unique *Xba*I site of pSP35-9ΔΩ. An orientation of this cloned fragment equal to the truncated *petH* gene on the construct was selected. The resulting construct was linearised with *Not*I before subsequent transformation.

2.4. Genetic construction of petH-gfp transcriptional and translational fusions

A fusion was made between the coding region of the N-terminal domain of *petH* with the *Aequorea victoria gfp* gene, encoding the Green Fluorescent Protein (GFP), resulting in a translational fusion construct. Likewise, a fusion was made of the *petH* promoter/operator (P/O) region to the *gfp* gene, resulting in a transcriptional reporter construct.

A 1.6 kbp *Eco*RI/*Sal*I fragment from pKOK6 [25] containing the *nptII* gene, encoding kanamycin resistance, and the phage fd bidirectional transcription terminator, was cloned into pBluescript SK+, and digested with *Eco*RI and *Sal*I. The resulting vector was digested with *Eco*RI and *Bam*HI, and ligated with the 0.8 kbp *Eco*RI/*Xba*I fragment from pGFPuv (Clontech) containing the *gfp*-uv gene, together with the 0.85 kbp *Xba*I/*Bam*HI fragment from pSP35-9 [15], encoding the *petH* P/O region and the N-terminal region of the *petH* gene. This allowed the in-frame fusion between the PetH N-terminal 75 residues, comprising the CpcD homologous domain [14], in frame with GFP, by ligation of the *Xba*I site present at the desired position in the *petH* gene, with the *Xba*I site present at the 5′ end of the *gfp-uv* gene. For the construction of the transcriptional fusion construct, the same fragments were ligated except for the 0.85 kbp *Xba*I/*Bam*HI fragment from pSP35-9, which was replaced by a 0.6 kbp *Xba*I/*Bam*HI digested PCR product generated with the M13REVERSE (5′-CAGGAAACAGCTATGAC-3′) and XBAPETPR (5′-GCTCTAGATACATGGGTTAATTGCTCCCTACTC-3′) oligonucleotides, with pSP35-9 as a template. This ligation allowed a fusion, directly downstream of the *petH* initiation codon with *gfp*, by use of the engineered *Xba*I site, resulting in a transcriptional fusion of *gfp* with the *petH* P/O region and Shine–Dalgarno sequence. Both constructs were transformed as circular DNA. Trans-

formants were selected as kanamycin resistant colonies.

It was noted that transformation of similar DNA constructs, based on the wild-type *Aequorea victoria gfp* gene, did repeatedly result in kanamycin resistant transformants with normal frequencies. However, those transformants could not be grown further than colonies or small-scale liquid cultures. Presumably, cytoplasmic wild-type GFP is toxic for *Synechocystis* cells, and segregation of the engineered genotype caused the arrest of growth.

Western blot analysis was performed with a mouse-α-GFP monoclonal antibody (Clontech) at 1:10,000 dilution. Detection was with chemiluminescent reagent SuperSignal (Pierce).

2.5. *In vivo assays of PS I-dependent cyclic electron transport: $P700^+$ re-reduction kinetics and photo-acoustic energy storage measurements*

Synechocystis cells (about 10 μg chlorophyll *a*) were deposited on a nitrocellulose membrane and illuminated with light specific for PS I (e.g., $\lambda > 715$ nm; far-red light). The formation of $P700^+$ was detected by the pulse-modulated measurement of the increase in absorbance at 820 nm [6]. The kinetics of the subsequent $P700^+$ re-reduction in the dark was taken as a measure for the capacity of PS I-dependent cyclic electron transport. Under these conditions electron donation by PS II did not significantly contribute to the rates obtained, since the addition of 5 μM DCMU did not influence the measurements. The rate of $P700^+$ re-reduction is usually given as the reaction half-time. However, we observed that this half-time is largely independent of the concentration of $P700^+$ that is accumulated during actinic illumination. This reaction can therefore mathematically be described as a (pseudo-) first-order reaction. Its rate constant k (s^{-1}) equals $\ln 2/t_{1/2}$.

The photo-acoustic measurement of PS I-dependent cyclic electron transport capacity also depends on the use of far-red light [5,6]. Cells (about 30 μg chlorophyll *a*) were packed on a Millipore nitrocellulose membrane with 3 μm pore size and a diameter of 12 mm by filtration and placed in the photo-acoustic chamber. The sample was illuminated with 8 W m^{-2} far-red light, modulated at a frequency of 20 Hz. The photo-acoustic signal was measured with a lock-in amplifier. PS I reaction centres were closed by illumination with 3000 μmol photons $s^{-1}\,m^{-2}$ white light. Under these conditions, the pulse-modulated measurement of heat release, produced by absorption of far-red light, was taken as 100% (i.e., the energy storage was 0%). Including DCMU at a concentration of 5 μM did not influence the measurements, demonstrating the specific excitation of PS I by far-red light. The photo-acoustic chamber was flushed with nitrogen to ensure that the terminal oxidase activity and photochemical side-reactions, such as reduction of oxygen, did not affect the level of the determination.

2.6. *Biological preparations, native PAGE and assays*

Cell-free extracts were prepared with a French Press (Aminco Corp, USA), operated at 20 000 psi (0°C) in a buffer containing 50 mM Tricine (pH 7.9), 10 mM NaCl, 5 mM $MgCl_2$ and 0.5 mM PMSF. Whole cells and cell debris were subsequently removed by centrifugation. Membranes were prepared by precipitation and collected by centrifugation after the addition of 1% (w/v) streptomycin sulfate. After two subsequent precipitations, membranes no longer contained detectable amounts of phycobilisomes. Cell-free extracts, thylakoid membranes and cytoplasmic fractions were loaded on native 12.5% acrylamide gels, containing 500 mM Tris/glycine (pH 8.8) and 0.05% Triton X-100. Phycobilisomes were prepared according to [26]. NADPH-dependent diaphorase activity was detected after electrophoresis by incubating the gel in a buffer containing 0.2 mg/ml nitrotetrazolium blue (NBT), 0.5 mM NADPH, 25 μg/ml glucose-6-P dehydrogenase, 5 mM glucose-6-P and 50 mM Tris–HCl, pH 8.0. Recombinant 47 kDa wild-type FNR and 38 kDa truncated FNR, lacking 75 N-terminal residues, were prepared as described previously [20].

Diaphorase assays for the quantification of FNR in subcellular fractions were performed essentially as in [15], with the exception of the pH of the TAPS (*N*-tris[hydroxymethyl]methyl-3-amino-propanesulfonic acid) buffer, which was 9.5, and the addition of 0.025% (v/v) Triton-X100 (Sigma), which destroys the diaphorase activity of the NAD(P)H dehydrogenase complex as it does in native gels. At pH 9.0 no influence on the diaphorase activity due to thyla-

koid association was observed, in accordance with previous observations with the chloroplast FNR [27,28].

Cell-free extracts and thylakoid membranes for Western analysis after sodium dodecyl sulfate–polyacrylamide gel electrophoresis (SDS–PAGE) were prepared using the same procedures. GFPuv and GFPuv fusion proteins were detected with a mouse-α-GFP monoclonal antibody (Clontech) at 1:10,000 dilution.

Chlorophyll *a* concentration was determined after extraction with methanol at room temperature of either a cell pellet, or of a concentrated thylakoid membrane preparation, according to [29].

2.7. Electron microscopy

Cells of *Synechocystis* PCC 6803 were fixed with 3% (w/v) glutaraldehyde in phosphate buffered saline, pH 7.5 (PBS), dehydrated in a graded ethanol series and embedded in Unicryl (BioCell). Ultra-thin cryo-sections were labelled with a 1:1000 dilution of a polyclonal rabbit-α-GFP antibody (Molecular Probes). The secondary antibody was a goat-α-rabbit 15 nm gold-labelled antibody (Amersham). The thin sections were negatively stained with 1% (w/v) uranyl acetate and examined with a Philips CM10 electron microscope. The primary antibody was incubated with a preparation of thylakoid membranes from wild-type *Synechocystis* PCC 6803 in order to reduce background labelling of the thylakoids.

3. Results and discussion

3.1. Induction of PS I-dependent cyclic electron transfer in Synechocystis PCC6803 after a salt shock is preceded by over-expression of petH mRNA

Changes in cyclic electron transfer capacity by the $P700^+$ re-reduction assay and the photo-acoustic energy storage assay have been recorded in conjunction with estimation of the expression level of *petH*. The adaptation after the addition of 0.55 M NaCl is completed in almost 8 h (Fig. 1). The increase in the energy storage capacity and the decrease in $P700^+$ re-reduction rate show identical kinetics. This sup-

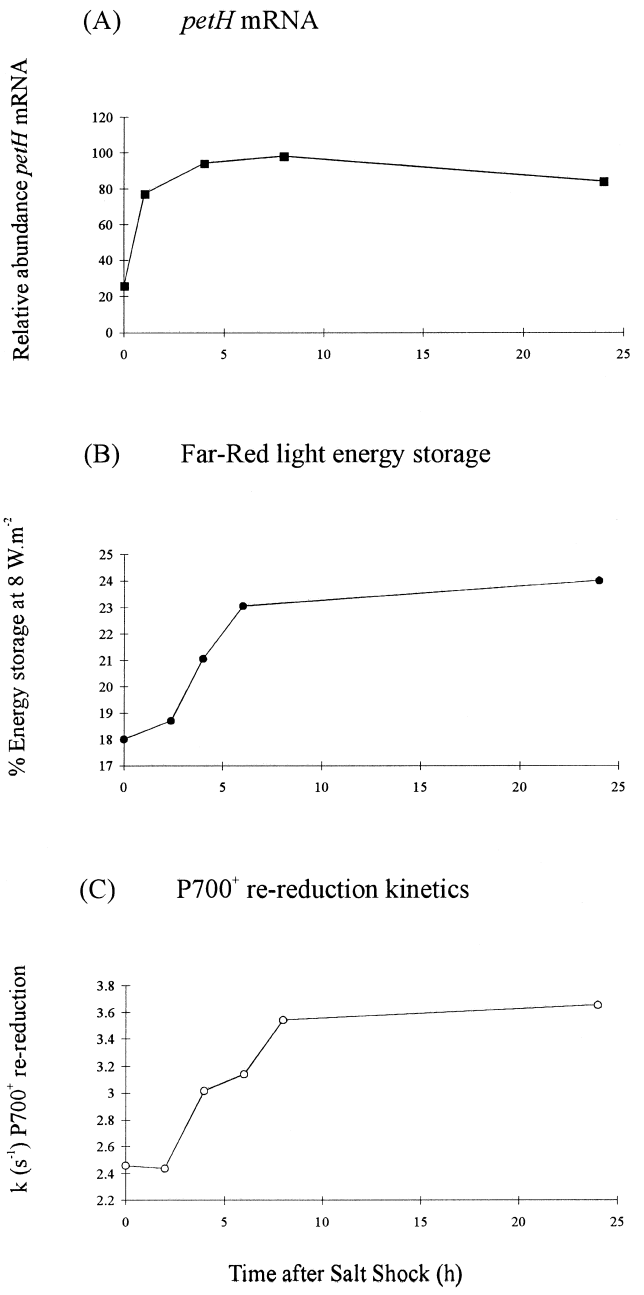

Fig. 1. Adaptation of *Synechocystis* PCC 6803 to a salt shock of 0.55 M NaCl. At time 0 h, NaCl was added at a concentration of 0.55 M. The capacity for cyclic electron transfer was regularly assayed during 25 h both by photoacoustic far-red light energy storage determinations and $P700^+$ re-reduction measurements. The accumulation of *petH* mRNA, encoding ferredoxin:$NADP^+$ reductase, was assayed at similar time intervals by Northern hybridisation. The relative transcript abundance was determined from the relative density of the hybridising bands, which was corrected for the total amount of RNA from ethidium bromide-stained gels.

ports our conclusion that both techniques monitor the same physiological rate limitation. Quantitative Northern blot analysis of the *petH* transcript shows that its over-expression precedes the increase in capacity of PS I cyclic electron transfer by approximately 2 h (Fig. 1). This might indicate a causal relation between the *petH* over-expression and maturation of the protein and the increase in capacity of the PS I cyclic electron transfer route.

3.2. Mutagenesis of petH: truncation of the N-terminal CpcD homologous domain

It was previously shown that a deletion of *petH* did not segregate [15]. Modification of the enzyme via deletion of the non-catalytic part of the protein was achieved through truncation of the N-terminal domain. That part of the FNR protein is homologous with the phycobilisome linker polypeptide CpcD. The procedure of integration of the construct is shown in Fig. 2. Double homologous recombination resulted in stable and fully segregated mutants with truncated *petH*. As a result the *prk–petH* intergenic region was duplicated. However, recombination at this site will lead to the loss of the only copy of the *petH* N-terminal coding sequence that was left in the mutant genome (Fig. 2). Complete segregation of the mutant genotype did not require selective growth conditions. The *petH* promoter region was characterised previously. Expression of *petH* showed regulation by light, and over-expression when cells were challenged with high salt [15]. For a correct study of the effect of the truncation of *petH* on cyclic electron transport, these transcriptional re-

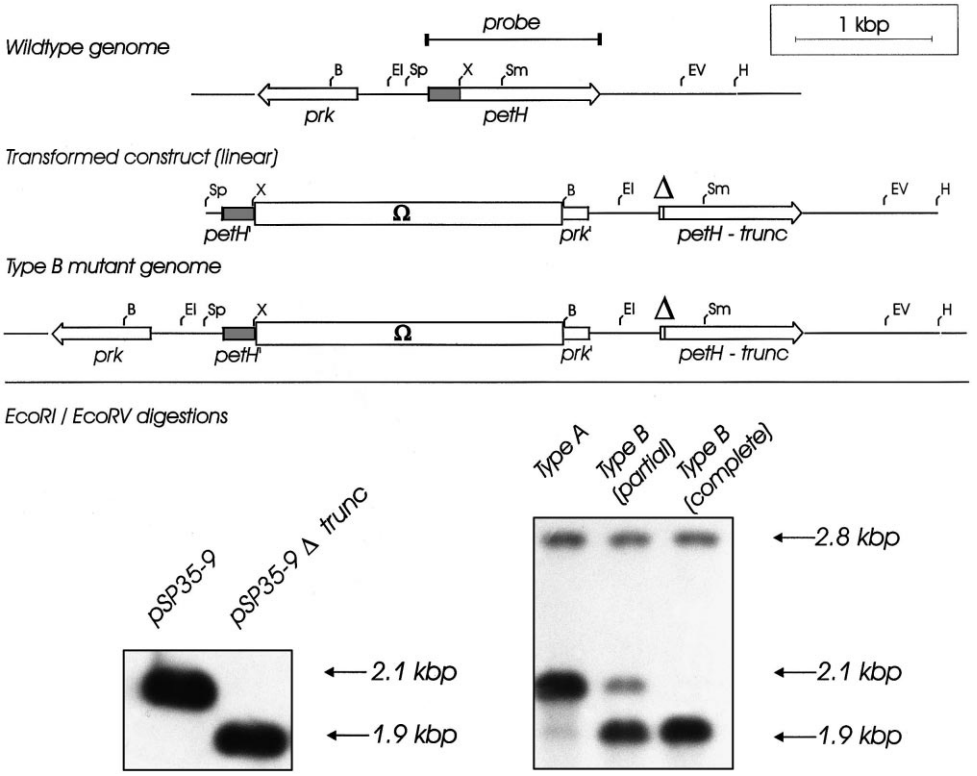

Fig. 2. Strategy and Southern analysis of replacement mutagenesis resulting in the 5′ in-frame deletion of 225 nucleotides from the open reading frame of *petH*. The gene organisation around *petH* is shown for the wild type. Restriction sites are indicated (B, *Bam*HI; EI, *Eco*RI; Sp, *Spe*I; X, *Xba*I; Sm, *Sma*I; EV, *Eco*RV; H, *Hin*dIII). The construct shown was linearised before transformation. Southern hybridisation analysis with the entire *petH* gene as a probe, is shown for *Eco*RI/*Eco*RV double digestions of genomic DNA and the controls, plasmids pSP35-9 and pSP35-9Δ trunc, containing the wild-type *petH* and the truncated Δ*petH* gene. The 'Type A' genotype resulted from integration of the marker via a recombination event upstream of the FNR N-terminal coding region. Replacement of the wild-type *petH* gene by the truncated Δ*petH* gene via recombination downstream of the deletion resulted in the mutant 'Type B' genotype.

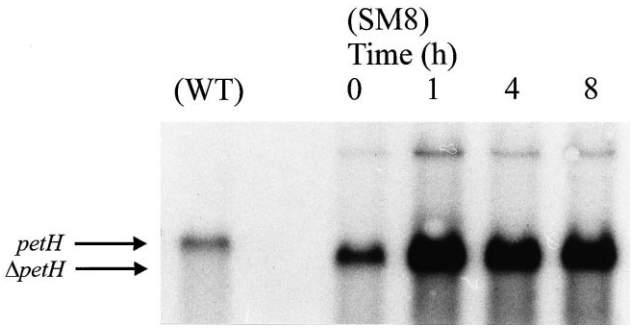

Fig. 3. Northern analysis of wild-type *petH* and accumulation after salt shock of Δ*petH* mRNA. Northern analysis of RNA from wild-type and SM8 'Δ*petH*' cells was performed with a *petH* DNA probe identical to the one used for Southern analysis (Fig. 2).

sponses had to be conserved. To test the confinement, 0.55 M NaCl was added to a growing culture of a mutant carrying the Δ*petH* gene, designated 'SM8'. The expression level of the truncated *petH* transcript was followed, during the subsequent hours, by Northern hybridisation. Over-expression in the mutant was observed already after 1 h. The increase in mobility of the 225 nucleotides truncated transcript is apparent (Fig. 3). Thus, salt stress mediated transcriptional regulation of the truncated gene is conserved in the mutant genotype. In addition, diaphorase activities determined in cell-free extracts of the wild type and the mutant, grown under standard conditions, were comparable.

3.3. Truncated FNR binds neither to thylakoid membranes nor to phycobilisomes

Wild-type and truncated FNR proteins were separated by native PAGE at pH 8.8. Relative rates of migration into the gel were detected by staining from catalytic activity after the electrophoresis (Fig. 4). Fractionation of the cell-free extract showed distribution of wild-type FNR over different pools, cytoplasm, membranes and phycobilisomes. As a result of the removal of the thylakoids the wild-type protein is no longer retarded in the gel and appears in the cytoplasm. This may suggest that the majority of the FNR molecules are associated with the membranes in suspension, even when Triton X-100 is present.

In the cell-free extract of the truncated mutant (SM8 lanes) FNR shows a high mobility (the faint one but lowest bands). The lowest band is related to PEST processed FNR, as is discussed below.

The stained bands at about one-third of the bottom of the frame are likely not related to FNR activity, since mobility is not affected by the truncation. In addition, these bands selectively disappear after one freeze–thaw cycle, which FNR withstands (data not shown). The *drgA* gene (slr1719 Cyanobase identifier) shows sequence homology to a nitroreductase, a NADH dehydrogenase, and a NAD(P)H-flavin oxidoreductase [30]. The *drgA* gene-product was recently identified in cell-free extracts of *Synechocystis* PCC 6803 to possess NADPH-dependent diaphorase activity, which can also be demonstrated in native gels [30], which makes the *drgA* gene product a likely candidate to cause the aspecific signal in Fig. 4. Activity of the NAD(P)H dehydrogenase complex was not detected in our gel system, presumably due to the presence of Triton X-100 in the gels. This conclusion was supported by the fact that cell-free extracts and thylakoid membranes from the NDH1 deficient mutant M55 produced the same bands as the wild type after activity staining of native gels (data not shown).

For comparison, the mobility profiles of the purified wild-type and the truncated recombinant proteins are also shown (right-hand-side frame). The mobility of both recombinant proteins is in agreement with the predicted pI and molecular masses. The calculated p*I* of the 47 kDa wild-type protein, based on the amino acid sequence, is 5.62, whereas the lowering to 4.99 for the 38 kDa truncated protein, is the result of the loss of the positively charged N-terminal domain. At pH 8.8 the charges are calculated to be −12.3 and −18.1, respectively. Fig. 4 shows that the truncated protein has a mobility that is 1.7 times faster than that of the wild-type protein, by consequence of both an increased charge and a decreased molecular mass of the truncated FNR.

The FNR concentration in cell-free extracts was estimated by measuring of the diaphorase activity at pH 9.5, in an assay with Triton X-100 included. The activity was calibrated by comparison with the activity of known quantities of the purified 47 kDa recombinant wild-type protein. The concentration was estimated to amount to 6.9 pmol FNR (μg Chl *a*)$^{-1}$, which corresponds to approximately 0.9 FNR

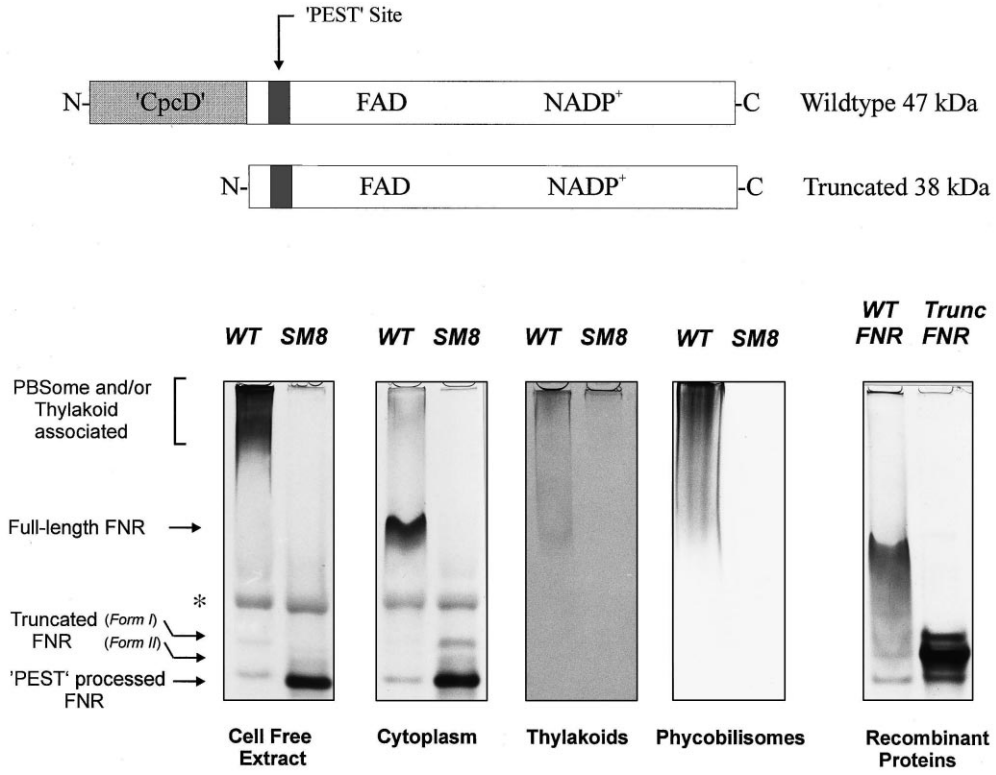

Fig. 4. Native gel electrophoresis and NADPH-NBT reductase activity staining. Native gel electrophoresis at pH 8.8 of cell fractions (for details see Section 2). Frames 1 to 4 show, from left to right, FNR activity for samples from wild-type and Δ*petH* truncation mutant SM8, in: frame 1, broken cell preparation; frame 2, cytoplasm after precipitation of membranes with streptomycin sulfate; frame 3, precipitated membranes; frame 4, isolated phycobilisomes; and frame 5, right, recombinant 47 kDa wild-type FNR and 38 kDa truncated FNR. 3 μg Chl *a* was loaded in the case of the cell-free extract and thylakoid preparations. The cytoplasmic fractions loaded were the equivalent of cell-free extracts (3 μg Chl *a*), after removal of the thylakoids by streptomycin sulfate precipitation. Five μg protein was loaded in the case of phycobilisome preparations, and approximately 100 ng protein was loaded in the case of the recombinant proteins. * Denotes aspecific stain development from the *drgA* gene product (see text).

per PS I. When thylakoids were precipitated with 1% (w/v) streptomycin sulfate twice, phycobilisome free membrane preparations were obtained. Only in wild-type membranes some FNR was retained after this treatment (Fig. 4). Quantification of the remaining thylakoid-bound FNR indicated presence of 0.9 pmol FNR (μg Chl *a*)$^{-1}$, which corresponds to an estimate of at least 0.12 FNR:PS I to be membrane associated in an amino-terminal extension requiring manner.

Preparations of phycobilisomes from wild-type *Synechocystis* PCC 6803 contain FNR, which is bound via the N-terminal CpcD-homologous domain [31,32]. It is calculated from the enzymatic activity present in such preparations that each phycobilisome complex contains approximately 2.4 copies of FNR. The native gel technique data in Fig. 4 demonstrate that FNR is no longer present in the gel lane with phycobilisomes of the SM8 mutant, since the phycobilisome-binding domain is removed from this protein.

The amount of FNR bound to isolated phycobilisomes relative to the concentration of FNR in cell-free extracts, allows to estimate that about 74% of the total pool of FNR molecules is bound to the phycobilisomes. The extinction coefficient at 625 nm for wild-type *Synechocystis* PCC 6803 phycobilisome complexes was determined to be approximately 29 500 mM^{-1} cm^{-1}, based on deconvoluted absorption spectra for phycocyanin chromophores [33] and the structural characterisation of the wild-type complexes [34]. Using this molar extinction coefficient, and assuming a Chl *a*:P700 ratio of 150:1, a phycobilisome:PS I ratio of 0.3:1 is determined from ab-

sorption spectra of whole cells. This is in reasonable agreement with the measured value of Ashby and Mullineaux [35]. The 2.4 copies of FNR per phycobilisome complex then correspond to 0.7 FNR:PS I. Thus, two independent types of calculation arrive at the conclusion that most of the FNR copies are bound to the phycobilisomes.

Both wild-type and recombinant proteins contain a highly mobile FNR fraction, which is most probably the result of proteolytic degradation (Fig. 4, bands with highest mobility). This band is present in wild-type and SM8 cell-free extracts and cytoplasm fractions and in preparations of recombinant proteins. Therefore, it is probably the result of N-terminal cleavage, yielding the same product in the case of both the wild-type and the truncated proteins. A potential cleavage site was found upon examination of the deduced amino acid sequence of PetH: a 'PEST-site' was detected at position 91–110 in the wild-type protein. This sequence (PSQSEGSGSEAVANPAPESN) is rich in proline, glutamic acid, serine and threonine residues. In addition, it is not too hydrophobic, and is flanked by (positively charged) lysine residues at both sides. These features are diagnostic for a PEST site. This particular site scored 7.33 with the algorithm of Rogers et al. [36], which is considered to be significant. This site is also present in the truncated protein, which lacks 75 N-terminal residues, at position 16–35. It cannot be predicted what the site of cleavage is based on the sequence only. However, the wild-type protein would probably gain most mobility after cleavage, since it would lose the positively charged N-terminal region. Note that in the original cell-free extract and in the cytoplasm fraction wild-type *Synechocystis* FNR, the contribution of PEST processed product is much less than in SM8. However, prolonged incubation at 0°C of the extract converted a significant fraction of the wild-type protein into the 'PEST-processed' species (data not shown). Others likely have detected exclusively proteolytically degraded FNR in extracts of *Synechocystis* PCC 6803 [30]. These authors determined the N-terminal sequence 'MTTTPKEK' (position 114–121 in the open reading frame). This N-terminus would result from cleavage at one residue on the C-terminal side of the positively charged lysine residue at position 112, that is part of the 'PEST' signature. We therefore suggest that the protein that was characterised in their study is identical to the 'PEST-processed' species that was observed in our native gels. A molecular mass of 34 kDa, a p*I* of 5.22, and a charge of −14 at pH 8.8 were calculated for this polypeptide.

Both the recombinant truncated protein and the protein present in the SM8 cell extracts are detected as a triplet. The band with the highest mobility has been assigned as a 'PEST-processed' species. The remaining doublet is assigned to truncated FNR. The nature of the difference in mobility between the two bands is not known.

3.4. *Green fluorescent protein attaches to thylakoid membranes and phycobilisomes only when fused to the N-terminal domain of FNR*

Fusions were made between the *Aequorea victoria gfp-uv* gene and both the promoter region of *petH* and the N-terminal 75 codons of *petH*, resulting in a transcriptional and a translational fusion construct, respectively. Both constructs were transformed to the wild-type *Synechocystis* PCC 6803 and the Δ*petH* truncation mutant 'SM8'. Transformants were selected for their kanamycin resistance.

Western blot analysis showed that both GFP itself and the 38 kDa PetH′–GFP fusion proteins were expressed in the kanamycin resistant transformants (Fig. 5A). Purified recombinant GFP was used as a marker for quantification (Fig. 5A, lane 1). Both in the wild-type and in the SM8 mutant background it was found that the PetH′–GFP fusion was more abundant in transformants than the corresponding, transcriptionally fused GFP. Additionally, it appeared that the abundance of both GFP and the fusion protein in SM8, was lower than in the wild-type background. Fluorescence of neither GFP nor the GFP fusion protein was observed by fluorescence spectroscopy, neither in cell suspensions nor in cell-free extracts. Since Western blot analysis of non-denatured samples showed that most GFP was present as the auto-oxidised species (data not shown), it was concluded that fluorescence was quenched in whole cells and in cell-free preparations.

When (phycobilisome-free) thylakoid membranes were prepared by two subsequent streptomycin sulfate precipitations, only the PetH′–GFP fusion protein was detected with the monoclonal antibody,

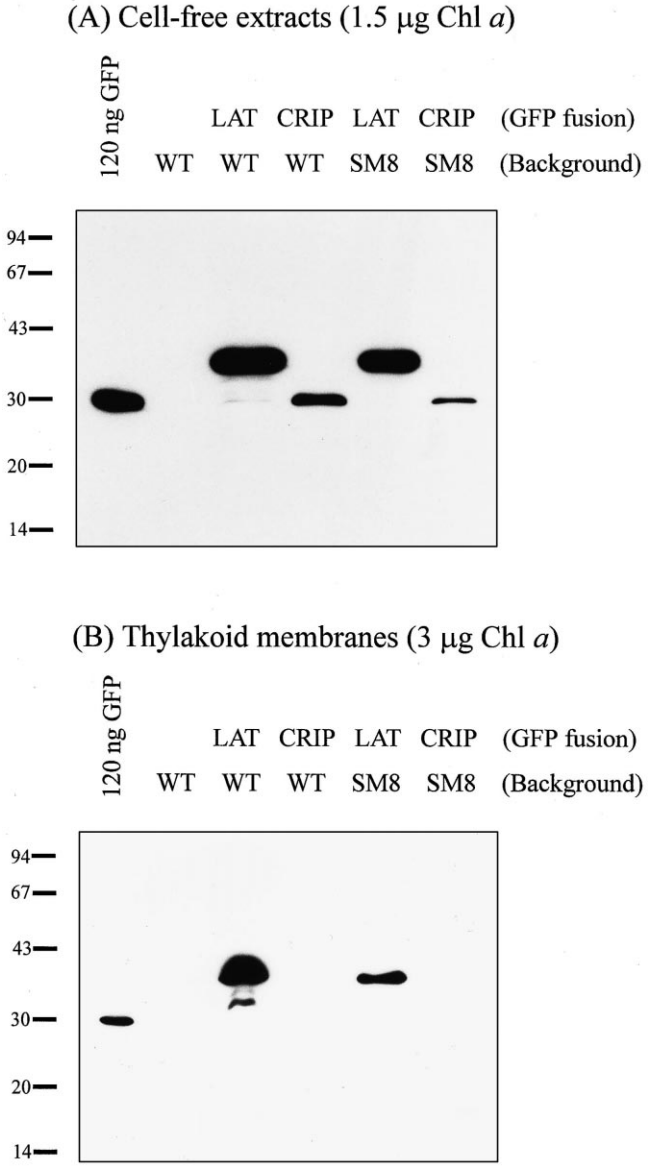

Fig. 5. Western detection of GFP and PetH′–GFP fusion proteins in recombinant *Synechocystis* strains. (A) GFP and GFP fusion proteins in cell-free extracts. Cell-free extracts (1.5 μg Chl *a*) were loaded per lane. 120 ng (3.75 pmol) recombinant purified GFPuv was loaded as a reference. Lane 2, wild type; lane 3, WT-GFPlat (translational GFP-fusion in wild-type background); lane 4, WT-GFPcript (transcriptional GFP-fusion in wild-type background); lane 5, SM8-GFPlat (translational GFP-fusion in SM8 background); lane 6, SM8-GFPcript (transcriptional GFP-fusion in SM8 background). (B) GFP and GFP fusion proteins in thylakoids. Phycobilisome-free thylakoid preparations (3 μg Chl *a*) were loaded per lane. 120 ng (3.75 pmol) recombinant purified GFPuv was loaded as a reference. Lane 2, wild type; lane 3, WT-GFPlat; lane 4, WT-GFPcript; lane 5, SM8-GFPlat; lane 6, SM8-GFPcript.

both in the case of the wild type and in the SM8 background (Fig. 5B). GFP from the WT-GFP and SM8-GFP transcriptionally fused strains do not co-purify with the thylakoids (Fig. 5B). This demonstrates independently of the properties of the domains common in wild-type and truncated FNR proteins, that the N-terminal domain of PetH is essential for the binding affinity of wild-type FNR onto the thylakoid membranes. Most PetH′–GFP fusion protein binds to thylakoid membranes: about 5.3 pmol (μg Chl *a*)$^{-1}$ (equivalent to approximately 0.7 GFP/PS I) in the case of the wild-type background. This is comparable to the amount of wild-type FNR present in thylakoid membranes. It is noted that most, or all,

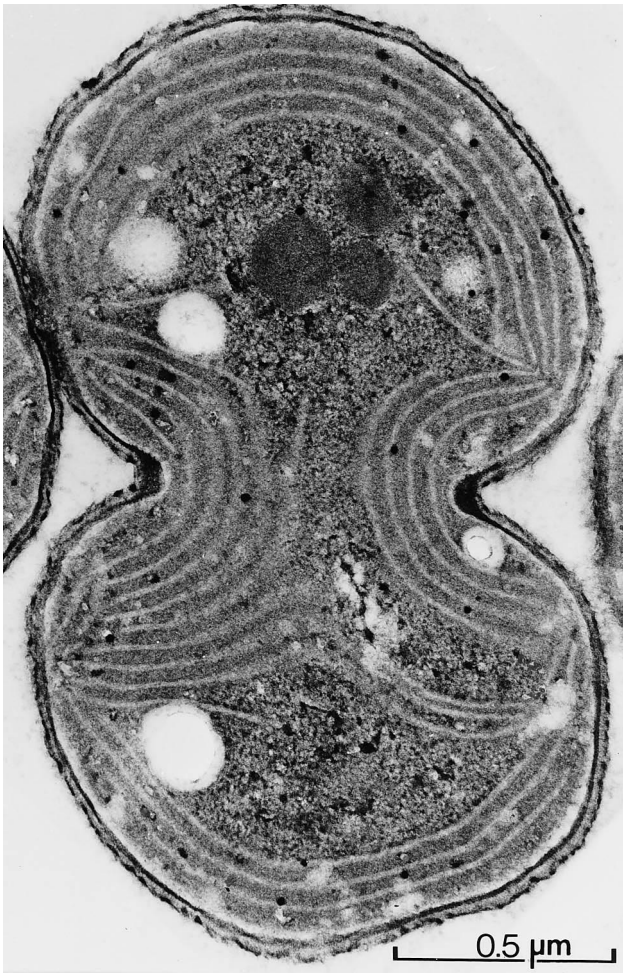

Fig. 6. In situ localisation of the GFP-fusion protein. Immunogold (15 nm) labelling of a thin section of glutaraldehyde fixed cells of the WT-GFPlat strain. An α-GFP polyclonal antibody was used at a 1:1000 dilution. The thin section was negatively stained with uranyl acetate. Bar = 0.5 µm.

fusion protein is recovered in the thylakoid membrane fraction. This is the case for both the wild-type and the SM8 mutant background. This suggests that there is no detectable competition for binding sites between FNR and the PetH′–GFP fusion protein. As expected, some fusion protein also co-purifies with the phycobilisome complexes, rendering proof for the phycobilisome-binding properties of the N-terminal domain as well [32].

Cells from the WT-GFP translational fusion strain were studied by immuno-gold labelling and subsequent analysis by electron microscopy. This rendered 'visible' evidence for the sub-cellular localisation of the PetH′–GFP fusion protein (Fig. 6). Using a polyclonal α-GFP antibody confirmed the specific labelling of the thylakoid membranes. However, some labelling of the thylakoid membranes in cells of wild-type *Synechocystis* PCC 6803, naturally without GFP protein, was also observed (data not shown). Western blot analysis identified an unknown component in the thylakoid membranes with a molecular mass of approximately 90 kDa. This rendered an explanation for the aspecific binding. Pre-incubation of the primary antibody with isolated thylakoid membranes from the wild-type strain increased the labelling specificity of the IGG. The average number of gold particles per cell in the wild type decreased to approximately 20–30% relative to the number of gold particles per cell of the WT-GFP translational fusion strain (data not shown). Hardly any labelling of the cytoplasm was observed, in accordance with Western blots that confirmed absence of GFP in cleared cell fractions of the recombinant strains with expression of PetH′–GFP fusion protein. From both of these in situ labelling- and cell-fractionation experiments we conclude that most of the fusion protein is attached to the thylakoid membranes, regardless of the presence of wild-type FNR. It was calculated that approximately 10% of the GFP fusion protein binds onto the phycobilisomes in the WT-GFP translational fusion strain. It is concluded that most of the molecules of the GFP fusion proteins are associated with the thylakoids via binding sites other than the phycobilisome complexes.

3.5. *Photo-acoustic- and P700$^+$ re-reduction measurements show that the N-terminal domain of PetH is required for salt-shock-inducible Photosystem I-dependent cyclic electron transfer capacity*

Adaptation to salt stress conditions results in an increase in the rate of PS I-dependent cyclic electron transfer. This inducible increase is largely independent of the NDH1 complex activity, as the phenomenon was observed in both the wild type and mutant M55 (Table 1; [12]). As different from the wild type and M55, mutant SM8, adapted to high salt, largely lacked the induction of cyclic electron flow capacity. It became concluded that even in the presence of functional NAD(P)H dehydrogenase complex, the

Table 1
Growth characteristics and PS I-dependent cyclic electron transfer measurements of wild-type, FNR-truncation mutant (SM8), NdhB-deficient (M55), and double mutant (FNR-truncated and NdhB-deficient mutant DM4) *Synechocystis* PCC6803 cultures in Normal and Salt added (0.55 M NaCl final) growth conditions

	Wild-type		SM8 (Δ*petH*)		M55 (*ndhB*$^-$)		DM4 (Δ*petH*+ *ndhB*$^-$)	
	Normal growth	Salt-added growth	Normal growth	Salt-added growth	Normal growth	Salt-added growth	Normal growth	Salt-added growth[a]
Growth rate (h)	5.5 ± 0.5	8.5 ± 0.5	5.5 ± 1	8.5 ± 1	6.5 ± 0.5	10.5 ± 0.5	6.5 ± 1	–
Energy storage (%)	18 ± 1.2	24 ± 1.7	16.5 ± 1.7	16.5 ± 1.7	7 ± 0.6	11 ± 1	3 ± 0.3	3 ± 0.3
$P700^+$ reduction (s^{-1})	2.31 ± 0.3	3.85 ± 0.3	2.24 ± 0.3	2.20 ± 0.3	0.71 ± 0.04	1.20 ± 0.06	0.69 ± 0.07	0.46 ± 0.05

Growth is given as the time (hrs) required for cell division under photoautotrophic growth conditions at 34°C, with continuous bubbling of 3% CO_2 in air. The capacity of PS I-dependent energy storage is the percentage of absorbed far-red light provided at 8 W m^{-2} that is converted into photochemical products. Rates of dark re-reduction of $P700^+$, acquired in 8 W m^{-2} far-red light, are given as pseudo-first-order reaction constants. Data for wild-type and mutant M55 cells were taken from [12], with permission.
[a]Measurements of $P700^+$ re-reduction and far-red light energy storage for salt-stressed cells of mutant DM4 were measured with a salt-adapted revertant of DM4; for details see text.

adaptation to 0.55 M NaCl mostly depends on a function of the N-terminal domain of FNR.

A phycocyanin deficient mutant '4R' [37] was also tested for its capacity of cyclic electron transport, and was found to closely resemble the wild type both with and without salt stress. Since preparations of the allophycocyanin core from this mutant lack substantial amounts of FNR, most probably no complex between FNR and the phycobilisome exists in vivo in this mutant, just as in mutant SM8. Since induction of cyclic electron transport due to salt stress is observed in mutant 4R, the fraction of the FNR molecules that is bound to the phycobilisomes is not responsible for the inducible function in increased cyclic electron transfer capacity.

The double mutant DM4 (carrying the M55 as well as SM8 mutation) did not grow under salt stress conditions, indicating that both NDH1 complex activity and wild-type FNR activity independently deliver an essential contribution to cyclic electron transport under salt stress conditions. After prolonged growth of the double mutant DM4 under standard photoautotrophic growth conditions, that is in the absence of added salt, it was found that suppressors arose that gained the ability to grow under salt stress conditions. A revertant of DM4 was tested for energy storage and $P700^+$ re-reduction kinetics. It was found that the energy storage in this revertant under standard conditions was higher than in the original double mutant. After cultivation of the revertant in high salt medium the energy storage capacity did not increase above the level obtained in the revertant culture without salt. The level of energy storage in the revertant was significantly lower than the level determined for the M55 single mutant (Table 1). The $P700^+$ re-reduction kinetics were comparable under standard conditions for M55 and the revertant of double mutant DM4, whereas the double mutant in high salt cultures showed significantly decreased rates of electron transport (Table 1). Presumably an additional route of plastoquinone reduction was induced in reverted DM4, that allowed growth under salt stress conditions. However, since this route was not induced under salt stress conditions, it did not involve the function of the salt stress-inducible wild-type FNR.

Photoautotrophic growth of mutant SM8 was comparable to that of wild-type cells, both in normal and salt stress conditions (Table 1), indicating that the PS I-dependent cyclic electron transport that is catalysed by FNR does not contribute significantly to growth when the NDH1 complex is present. An effect of the FNR truncation on growth could only be observed in the DM4 double mutant (no growth), if cells were challenged with salt.

4. General discussion

Previous studies have indicated that the N-terminal domain of *Synechocystis* FNR plays no role in linear photosynthetic electron transfer [20]. In addi-

tion, the binding of FNR to the phycobilisomes via this domain does not enhance the energy transfer capacity of those light harvesting complexes to neither the PS II nor the PS I reaction centres [32]. In contrast to the two former studies the present work has disclosed an actual function for the N-terminal domain. We have shown correlation between the binding of FNR to the thylakoid membranes via its N-terminal domain and increased capacity for PS I-dependent cyclic electron transfer.

The distribution of FNR in *Synechocystis* PCC 6803 is in three pools. Three quarters of the total pool is present in the phycobilisomes. Under conditions of salt stress the FNR level increases, and the additional molecules are associated with 'reverse' electron transfer to plastoquinone, a quinone/cytochrome-b_6f reductase function, which is a basic requisite for PS I cyclic electron transfer. It was found that a specific interaction of the N-terminal domain with the thylakoid membrane directs the copies that are not bound to the phycobilisomes to the thylakoid membrane. In agreement with these results it was shown by analysis of isolated subcellular fractions, and in situ localisation experiments, that a fusion protein of GFP with the N-terminal domain of FNR, also binds to the thylakoid membranes.

Two modes of interaction, that are only detected for the 47 kDa wild-type protein with the thylakoid membrane, seem apparent from the native gel experiments and accomplished FNR quantification. One mode is tight interaction that allows co-purification of FNR with the membrane fraction, when using a streptomycin sulfate precipitation protocol. These copies represent a small fraction of the FNR pool. The other mode of interaction is an association with unknown thylakoid components that can exist in the presence of Triton X-100, but is broken during precipitation of the membranes with streptomycin sulfate, and presumably relies on a modification of the N-terminal domain. In wild-type cells, most of the FNR is present as the 47 kDa full-length species, although cleavage at a 'PEST' site yields small amounts of a processed species that lacks the N-terminal CpcD homologous domain. Interestingly, a PEST site can also be detected in the deduced amino acid sequence of the *Synechococcus* sp. PCC 7002 FNR [31].

The M55 mutant lacking the NDH1 complex and a PsaE-deficient mutant have been examined for this interaction, and were found to show wild-type FNR-thylakoid interactions (data not shown). These controls indicate binding of FNR to the thylakoid membranes independent of the NDH1 and PsaE proteins. The conclusion is that the N-terminal CpcD homologous domain constitutes a thylakoid binding domain, as well as a phycobilisome binding domain. When cell-free extracts of the wild type are prepared in low ionic strength buffers, phycobilisome-associated FNR is released and shows affinity for the thylakoid, in contrast to the truncated protein. Copies of FNR that are not associated to the phycobilisome complexes are firmly bound to the thylakoid membranes via the N-terminal CpcD homologous domain, and are recovered in the membrane fraction, whereas the bulk of the FNR protein is not. An additional experiment showed that membranes isolated from a sucrose step-gradient after ultracentrifugation [38] contain about 70% of the enzymatic (diaphorase) activity that is present in membranes from a cell-free extract. This contrasts with lack of FNR association to thylakoids from mutant SM8, the membranes of which otherwise demonstrate affinity for binding of wild-type FNR (data not shown).

Measurements of far-red light energy storage capacity and assays of $P700^+$ re-reduction indicate that in the SM8 mutant induction of cyclic electron flow capacity by salt shock is absent. This inducible flux of cyclic electron transfer correlated with over-expression of FNR in the wild-type strain [15]. As a result of salt shock the FNR concentration increases above the level that is normally present in the phycobilisomes, providing a clue towards a possible mechanism for control of the pool size that can engage either in 'linear' or in 'cyclic' electron flow. Ferredoxin:$NADP^+$ oxidoreductase activity in the sense of NADPH synthesis is associated with linear photosynthetic electron transfer, FNR:plastoquinone oxidoreductase activity is instrumental in PS I driven cyclic photosynthetic electron flow. The binding of FNR to the phycobilisome might in prospect simply constitute a mechanism that prevents the binding of FNR to the thylakoids and participation in plastoquinone/cytochrome-b_6f reductase activity. Since the FNR:phycobilisome and the phycobilisome:PS I ra-

tios are relatively constant, this could ensure that enough copies are present to catalyse linear electron transport. Accumulation of FNR, above the fixed level of presence in the phycobilisomes, is presumably the result of a specific transcriptional induction of the *petH* promoter [15]. This could in retrospect regulate the number of molecules that are available for PS I cyclic electron flow. The precise mechanism through which FNR contributes to PS I cyclic electron flow still awaits to be disclosed. During cyclic electron transfer, in vivo FNR could most probably catalyse ferredoxin-dependent (and/or flavodoxin-dependent) plastoquinone reduction. NADPH:plastoquinone oxidoreductase activity of FNR in PS I cyclic electron transfer through which FNR essentially is rendering $NADP^+$, is the reverse of its function in linear photosynthetic electron transfer. Whether ferredoxin or flavodoxin are intermediates, or whether the plastoquinone-cytochrome b_6f part of the cyclic electron flow is directly reduced by FNR remains to be answered. Note however, that the free energy difference between the ferredoxin (flavodoxin)/plastoquinone couple (−500 and −450 mV, respectively) is higher than between the NADPH/plastoquinone couple (−420 mV). Such electron donation to the plastoquinone may also be functional in dark oxidative respiration. In agreement with the original observation in [9] it was noted that the respiratory oxygen consumption rate of mutant M55 in the dark was significantly lower than that of the wild-type control. However, some 20–30% of the electron transfer rate remained present. This is pointing to the presence of mechanisms of plastoquinone reduction in intact cells of *Synechocystis* that proceed in another way than through the NDH1 NAD(P)H dehydrogenase complex activity.

The double mutant DM4, lacking both the NDH1 complex and the N-terminal domain of FNR, showed both the decreased capacity for cyclic electron transport (which is also observed for mutant M55) and the absence of induction of PS I cyclic after salt shock, by consequence of the truncation of FNR. Initially this double mutant strain did not grow in high salt media. However, revertants were selected under normal photoautotrophic conditions. A possible candidate for the alternative electron transfer pathway is NDH2, for which three putative genes have been identified in the genome sequence of *Synechocystis* PCC 6803: slr1743, slr0851 and sll1484 [39]. However, it was recently shown that these gene-products do not significantly contribute to plastoquinone reduction [40]. Instead, it is proposed that the succinate dehydrogenase complex contributes to the reduction of the plastoquinone b6f domain of *Synechocystis* in the DM4 revertants.

This is the first report that demonstrates the involvement of FNR in PS I-dependent cyclic electron flow without use of inhibitors or modifying agents as was the case in other studies with chloroplasts or cyanobacteria [16,17,41,42]. Instead the work presented is based on the characterisation of the phenotype of a mutant that was genetically engineered. In addition, this phenotype revealed tight association of FNR to the thylakoid membrane, via its CpcD-homologous N-terminal domain. Since the mechanism of thylakoid interaction is fundamentally different in the case of chloroplast FNR, in which a binding protein has been proposed [28,43], our results may not directly relate to PS I cyclic electron transfer operation in plants.

Acknowledgements

We acknowledge the expert technical assistance of Hans Balke and Betsie Voetdijk. We are grateful to Prof. L.K. Anderson for the gift of mutant 4R. A *ndhB* deficient mutant M55, lacking functional NAD(P)H dehydrogenase complex, was kindly provided by Dr. Ogawa [9].

References

[1] D.S. Bendall, R.S. Manasse, Biochim. Biophys. Acta 1229 (1995) 23–38.
[2] G. Schmetterer, in: D.A. Bryant (Ed.), The Molecular Biology of Cyanobacteria, Kluwer Academic, Dordrecht, 1994, pp. 409–435.
[3] P.C. Maxwell, J. Biggins, Biochemistry 15 (1976) 3975–3981.
[4] M. Nanba, S. Katoh, Biochim. Biophys. Acta 725 (1983) 272–279.
[5] S.K. Herbert, D.C. Fork, S. Malkin, Plant Physiol. 94 (1990) 926–934.
[6] J. Ravenel, G. Peltier, M. Havaux, Planta 193 (1994) 251–259.
[7] T. Endo, H. Mi, T. Shikanai, K. Asada, Plant Cell Physiol. 38 (1997) 1272–1277.

[8] H.B. Teicher, H.V. Scheller, Plant Physiol. 117 (1998) 525–532.
[9] T. Ogawa, Proc. Natl. Acad. Sci. USA 88 (1991) 4275–4279.
[10] H. Mi, T. Endo, U. Schreiber, K. Asada, Plant Cell Physiol. 33 (1992) 1099–1105.
[11] H. Mi, T. Endo, U. Schreiber, T. Ogawa, K. Asada, Plant Cell Physiol. 33 (1992) 1233–1237.
[12] R. Jeanjean, S. Bédu, M. Havaux, H.C.P. Matthijs, F. Joset, FEMS Microbiol. Lett. 167 (1998) 131–137.
[13] M. Hageman, L. Wölfel, B.J. Krüger, Gen. Microbiol. 136 (1990) 1393–1399.
[14] M. Hagemann, R. Jeanjean, S. Fulda, M. Havaux, F. Joset, N. Erdmann, Physiol. Plant. 105 (1999) 670–678.
[15] J.J. van Thor, K.J. Hellingwerf, H.C.P. Matthijs, Plant Mol. Biol. 36 (1998) 353–363.
[16] Y. Shahak, D. Crowther, G. Hind, Biochim. Biophys. Acta 636 (1981) 234–243.
[17] J.P. Hosler, C.F. Yocum, Biochim. Biophys. Acta 808 (1985) 21–31.
[18] L. Gonzalez de la Vara, C. Gomez-Lorejo, Photosynth. Res. 8 (1986) 65–78.
[19] S. Scherer, I. Alpes, H. Sadowski, P. Böger, Arch. Biochem. Biophys. 267 (1988) 228–235.
[20] J.J. van Thor, T.H. Geerlings, H.C.P. Matthijs, K.J. Hellingwerf, Biochemistry 38 (1999) 12735–12746.
[21] R. Rippka, J. Deruelles, J.B. Waterbury, M. Herdman, R.Y. Stanier, J. Gen. Microbiol. 111 (1979) 1–61.
[22] H.B. Pakrasi, J.G.K. Williams, C.J. Arntzen, EMBO J. 7 (1988) 325–332.
[23] T.A. Kunkel, J.D. Roberts, R.A. Zakour, in: R. Wu. (Ed.), Methods in Enzymology, vol. 154, 1987, p. 367.
[24] P. Prentki, H.M. Kirsch, Gene 29 (1984) 303–313.
[25] W. Kokotek, W. Lotz, Gene 84 (1989) 467–471.
[26] A. Glazer, Methods Enzymol. 167 (1988) 304–312.
[27] D.J. Davis, A. San Pietro, Arch. Biochem. Biophys. 184 (1977) 572–577.
[28] H.C.P. Matthijs, S.J. Coughlan, G. Hind, J. Biol. Chem. 261 (1986) 12154–12158.
[29] A.E.H. Marker, Freshwat. Biol. 2 (1972) 361–385.
[30] M. Matsuo, T. Endo, K. Asada, Plant Cell Physiol. 39 (1998) 263–267.
[31] W.A. Schluchter, D.A. Bryant, Biochemistry 31 (1992) 3092–3102.
[32] J.J. van Thor, O.W.M. Gruters, H.C.P. Matthijs, K.J. Hellingwerf, EMBO J. 18 (1999) 4128–4136.
[33] A.A. Demidov, M. Mimuro, Biophys. J. 68 (1995) 1500–1506.
[34] W.A. Sidler. in: D.A. Bryant (Ed.), The Molecular Biology of Cyanobacteria, Kluwer Academic, Dordrecht, 1994, pp. 139–216.
[35] M.K. Ashby, C.W. Mullineaux, Photosynth. Res. 61 (1999) 169–179.
[36] S. Rogers, R. Wells, M. Rechsteiner, Science 234 (1986) 364–368.
[37] T. Plank, C. Toole, L.K. Anderson, J. Bacteriol. 177 (1995) 6798–6803.
[38] T. Omata, N. Murata, Plant Cell Physiol. 24 (1983) 1101–1112.
[39] T. Kaneko, S. Sato, H. Kotani, A. Tanaka, E. Asamizu, Y. Nakamura, N. Miyajima, M. Hirosawa, M. Sugiura, S. Sasamoto, T. Kimura, T. Hosouchi, A. Matsuno, A. Muraki, N. Nakazaki, K. Naruo, S. Okumura, S. Shimpo, C. Takeuchi, T. Wada, A. Watanabe, M. Yamada, M. Yasuda, S. Tabata, DNA Res. 3 (1996) 185–209.
[40] C.A. Howitt, P.K. Udall, W.F.J. Vermaas, J. Bacteriol. 181 (1999) 3994–4003.
[41] J.D. Mills, D. Crowther, R.E. Slovacek, G. Hind, R.E. McCarthy, Biochim. Biophys. Acta 547 (1979) 127–137.
[42] R. Jeanjean, J.J. Van Thor, M. Havaux, F. Joset, H.C.P. Matthijs, in: Peschek et al. (Eds.), The Phototrophic Prokaryotes, Kluwer/Plenum, New York, 1999, pp. 251–258.
[43] E.A. Ceccarelli, R.L. Chan, R.H. Vallejos, FEBS. Lett. 190 (1985) 165–168.